Table S1. Data on human brain tissue analyzed in Figure 1. Beclin 1 levels did not correlate with either age or PMT. There was no significant difference in Beclin 1 levels between males and females. PMT; Time to Post Mortem (hours), MMSE; Mini Mental State Evaluation, C; non-demented control, AD; Alzheimer's disease, MCI; Mild Cognitive Impairment, LBV; Lewy Body variant of AD, HD; Huntington's disease, n/a; not available. Values are mean ± SE.

Diagnosis	n	Age	MMSE	PMT
C	19	75.4 ± 2.7	28.1 ± 0.8	7.7 ± 1.1
AD	16	80.5 ± 2.6	3.8 ± 1.3	7.7 ± 1.0
MCI	11	85.0± 2.7	28.8 ± 0.4	n/a
LBV	5	83.2 ± 1.0	14.0 ± 4.7	2.3 ± 1.0
HD	7	54.7 ± 6.0	n/a	8.6 ± 1.3

Table S2. Relative size of hippocampus and motor cortex in 9-month-old female mice were unchanged by beclin 1 deficiency. No significant differences were observed between the groups (t-test). Digitized images from 3-6 coronal sections (30 μm) at 360 μm intervals through the region of interest were captured and analyzed using Metamorph software. The region of interest (hip; hippocampus, mt ctx; motor cortex) was outlined, and the mean total number of pixels calculated. The investigator was blinded to genotype.

Genotype	Region	N	Mean area (pixels ± SEM)
APP^{+}, $Becn1^{+/+}$	mt ctx	7	1082641 ±26062
APP^{+}, $Becn1^{+/-}$	mt ctx	8	1052164 ± 15265
APP^{+}, $Becn1^{+/+}$	hip	6	780864 ± 38376
APP^{+}, $Becn1^{+/-}$	hip	8	878921 ± 37726

Figure S1. Beclin 1 immunoreactivity in sections from mid-frontal cortex of control and AD patients. Adjacent sections were stained with Cresyl violet to show neuron number. I-VI signify Braak stages of the representative AD cases, from mild (I), to severe (VI).

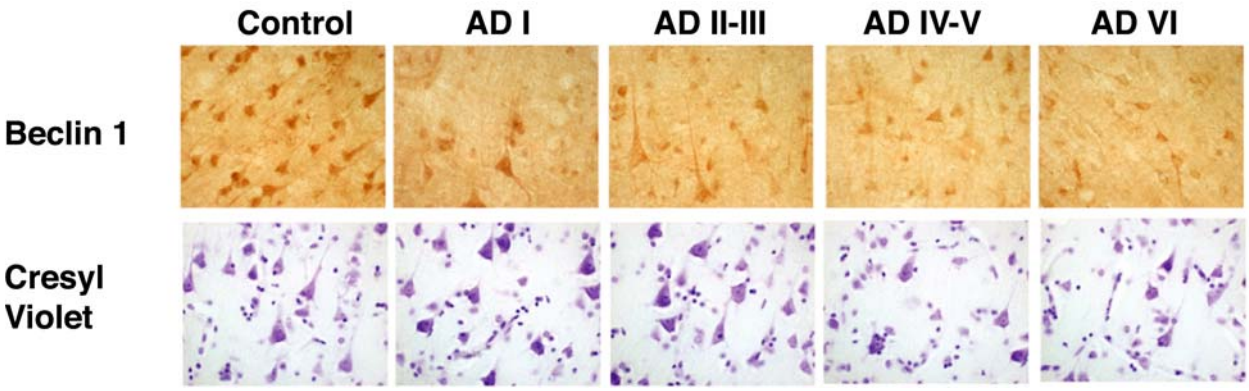

Figure S2. APP and CTF levels are equivalent in young *APP, Becn1*$^{+/+}$ and *APP, Becn1*$^{+/-}$ mice. APP (**A, B**), CTFβ (**A, C**), and CTFα levels (**A, D**) in the neocortex of 3-month-old *APP, Becn1*$^{+/+}$ mice (n = 3) and *APP, Becn1*$^{+/-}$ mice (n = 4). A representative western blot from replicate experiments (**A**) was probed with APP, CTF, and Actin antibodies. APP bands were normalized to Actin (**B**). CTF bands from the same samples on an independent blot were also normalized to Actin (**C, D**). All bars are mean ± SEM; mean differences were compared by unpaired Student's *t* test.

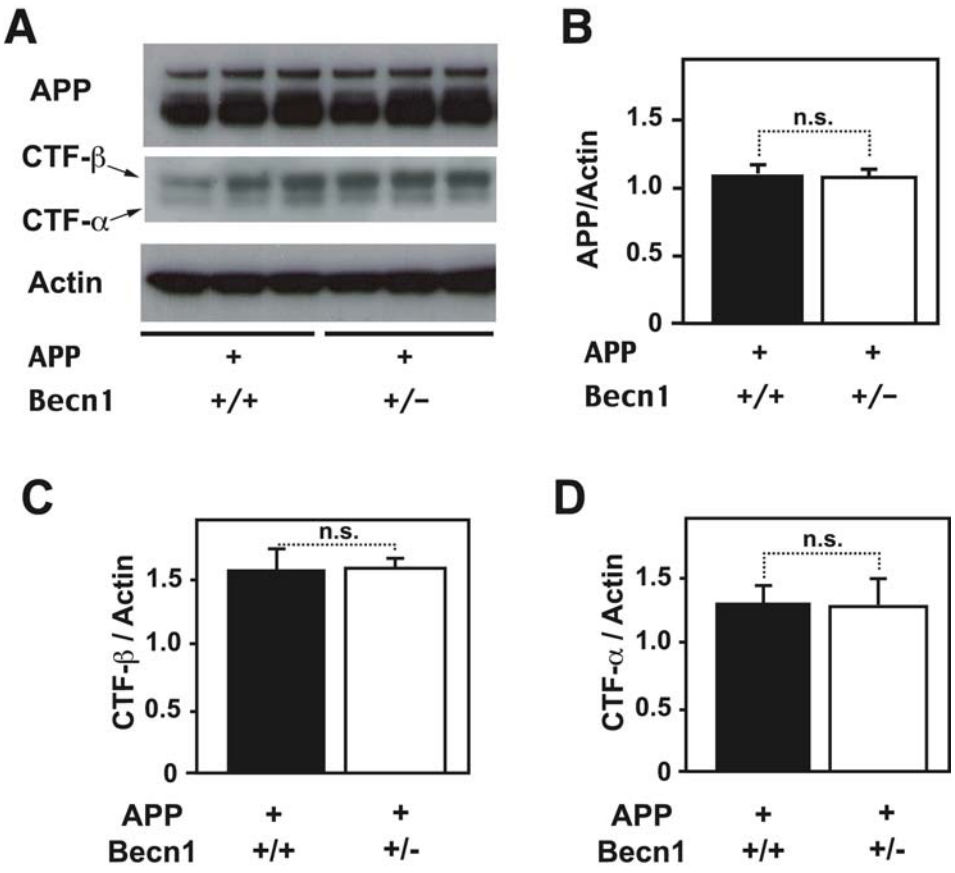

Figure S3. Distinct staining patterns in APP transgenic brains with antibodies detecting the APP holoprotein or Aβ. (**A, B**) Neocortex from nontransgenic mice (Non-tg) or 3, 6, and 12-month-old mice stained with antibodies recognizing human $A\beta_{17\text{-}24}$ (**A, B**) or human $APP_{444\text{-}592}$ (**C, D**). While Aβ immunostaining accumulates with age, APP immunostaining does not change or decreases slightly with age.

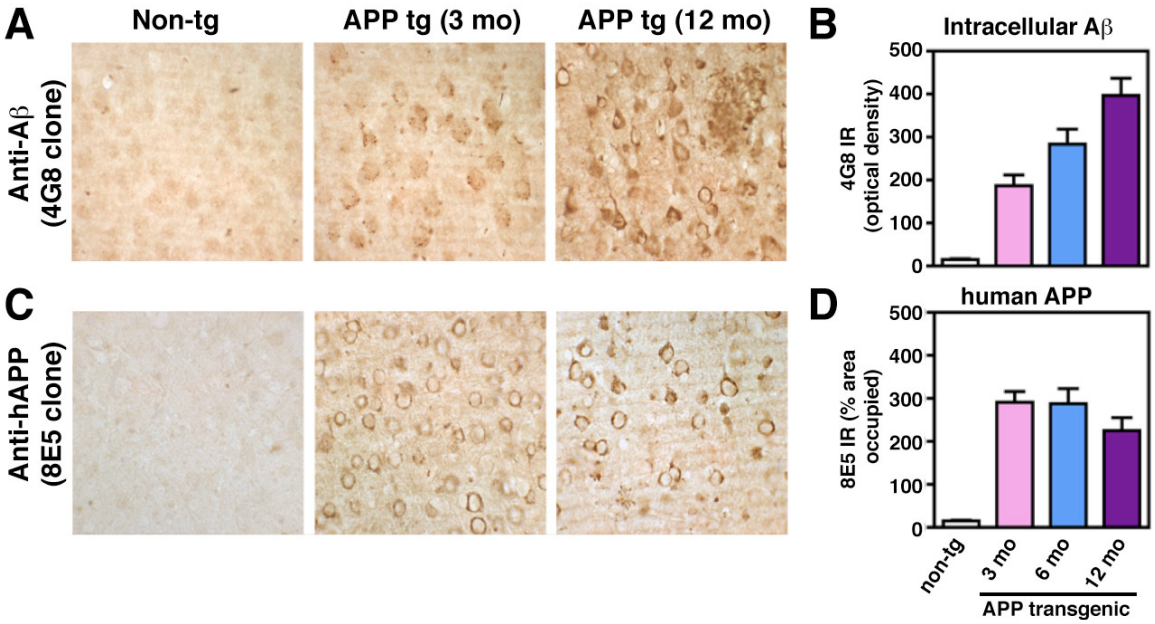

Figure S4. Intracellular Aβ is partially colocalized with Cathepsin D. (**A-D**) brain sections from a 9-month-old APP transgenic mouse were treated with formic acid to reveal intracellular Aβ and stained with antibodies against 4G8 ($A\beta_{17-24}$; **B, C**) or 3D6 ($A\beta_{1-5}$; **D**). Both antibodies show a granular intracellular staining pattern in neurons (**B, D**). Double staining with an antibody against cathepsin D (**A**) shows partial colocalization with Aβ (arrows). Scale bars represent 20 μm.

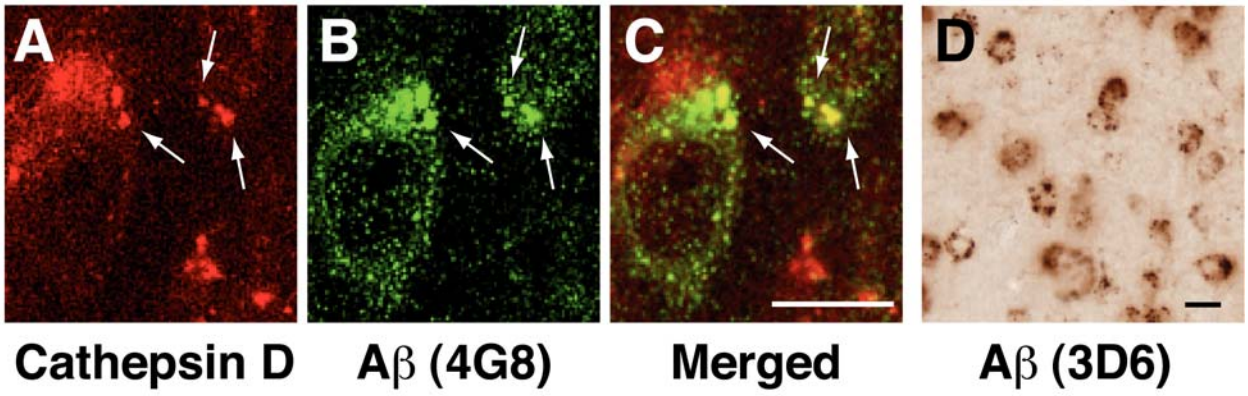

Figure S5. Additional ultrastructural disruptions in APP+, Becn1+/- mice. Lamellar bodies accumulated at synapses (arrowheads). Additional autophagosome like laminar bodies were identified (double arrowheads). Further pathological structures included fibrils (arrows) and electron dense bodies in axons (double arrows)